

Journal Pre-proof

Isotopic and microbial evidence for biodegradation of diluted bitumen in the unsaturated zone

Leah M. Mindorff, Nagissa Mahmoudi, Scott L.J. Hepditch, Valerie S. Langlois, Samrat Alam, Richard Martel, Jason M.E. Ahad



PII: S0269-7491(23)00172-0

DOI: <https://doi.org/10.1016/j.envpol.2023.121170>

Reference: ENPO 121170

To appear in: *Environmental Pollution*

Received Date: 24 October 2022

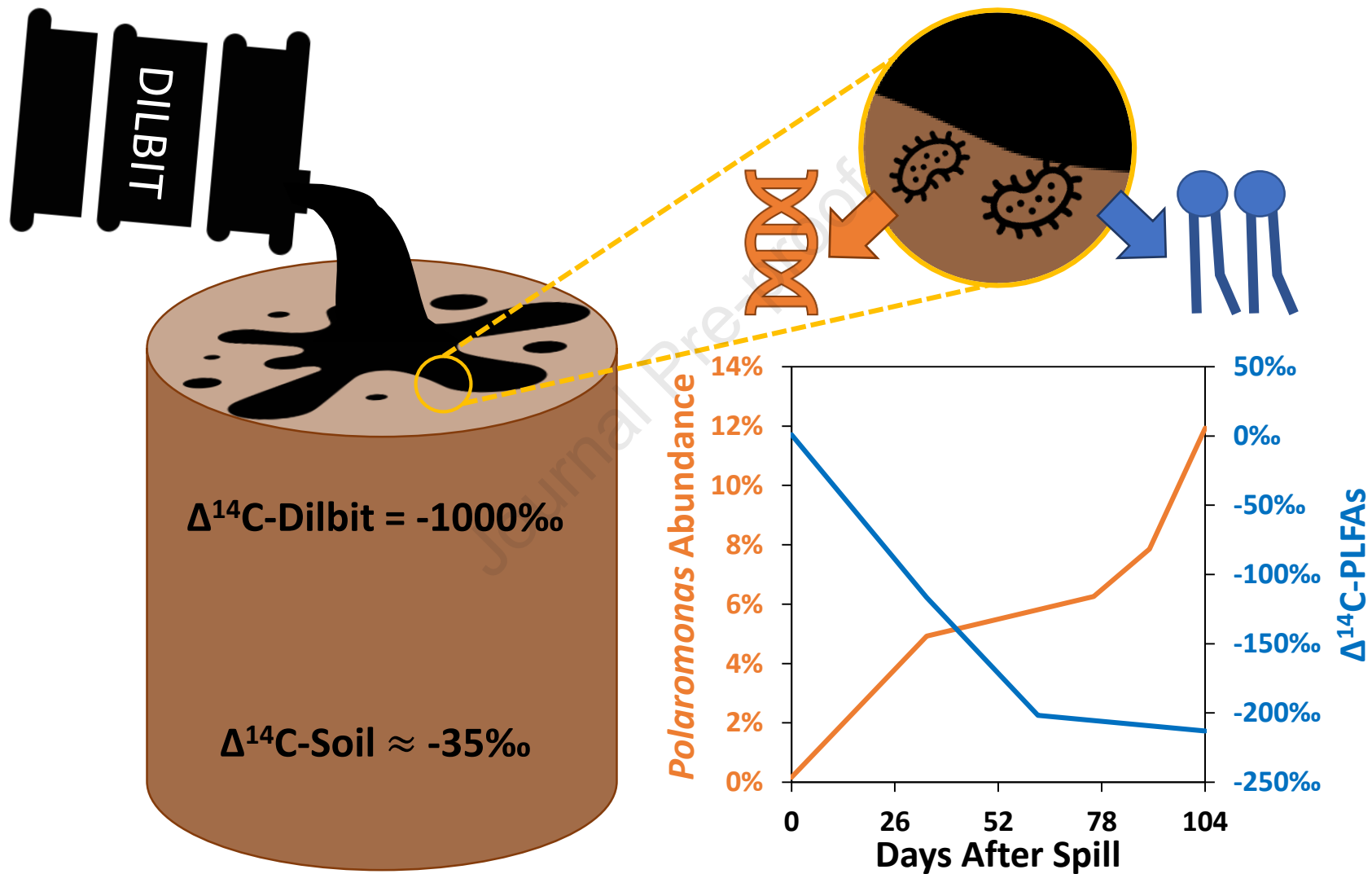
Revised Date: 23 January 2023

Accepted Date: 28 January 2023

Please cite this article as: Mindorff, L.M., Mahmoudi, N., Hepditch, S.L.J., Langlois, V.S., Alam, S., Martel, R., Ahad, J.M.E., Isotopic and microbial evidence for biodegradation of diluted bitumen in the unsaturated zone, *Environmental Pollution* (2023), doi: <https://doi.org/10.1016/j.envpol.2023.121170>.

This is a PDF file of an article that has undergone enhancements after acceptance, such as the addition of a cover page and metadata, and formatting for readability, but it is not yet the definitive version of record. This version will undergo additional copyediting, typesetting and review before it is published in its final form, but we are providing this version to give early visibility of the article. Please note that, during the production process, errors may be discovered which could affect the content, and all legal disclaimers that apply to the journal pertain.

© 2023 Published by Elsevier Ltd.



1 **Isotopic and microbial evidence for biodegradation of diluted bitumen in the**
2 **unsaturated zone**

3
4
5 Leah M. Mindorff^{1,2}, Nagissa Mahmoudi¹, Scott L. J. Hepditch³, Valerie S. Langlois³, Samrat
6 Alam², Richard Martel³, Jason M.E. Ahad^{2*}

7
8
9 1. Department of Earth and Planetary Sciences, McGill University, Montréal, QC, H3A 0E8,
10 Canada

11 2. Geological Survey of Canada, Natural Resources Canada, Québec, QC, G1K 9A9, Canada

12 3. Institut national de la recherche scientifique (INRS), Centre Eau Terre Environnement,
13 Québec, QC, G1K 9A9, Canada

14
15
16 * Corresponding author E-mail: jason.ahad@nrcan-rncan.gc.ca

17
18 **KEYWORDS.** Dilbit, crude oil, carbon isotopes, microbial communities, vadose zone,
19 groundwater

20
21
22
23 Final revision submitted to: *Environmental Pollution*, 23 January 2023

24 **Abstract**

25 The oil sands region in Western Canada is one of the world's largest proven oil reserves.
26 To facilitate pipeline transport, highly viscous oil sands bitumen is blended with lighter
27 hydrocarbon fractions to produce diluted bitumen (dilbit). Anticipated increases in dilbit
28 production and transport raise the risk of inland spills. To understand the behavior of dilbit in the
29 unsaturated or vadose zone following a surface spill, we ran parallel dilbit and conventional heavy
30 crude exposures, along with an untreated control, using large soil-filled columns over 104 days.
31 Phospholipid fatty acids (PLFAs), biomarkers for the active microbial population, were extracted
32 from column soil cores. Stable carbon isotope contents ($\delta^{13}\text{C}$) of individual PLFAs and
33 radiocarbon contents ($\Delta^{14}\text{C}$) of bulk PLFAs were characterized over the course of the experiment.
34 The $\Delta^{14}\text{C}$ -PLFA values in soils impacted by dilbit (-221.1 to -54.7‰) and conventional heavy
35 crude (-259.4 to -97.9‰) indicated similar levels of microbial uptake of fossil carbon. In contrast,
36 $\Delta^{14}\text{C}$ -PLFA values in the control column (-46.1 to +53.7‰) reflected assimilation of more recently
37 fixed organic carbon. Sequencing of 16S ribosomal RNA genes extracted from soil cores revealed
38 a significant increase in the relative abundance of *Polaromonas*, a known hydrocarbon-degrader,
39 following exposure to both types of oil. This study demonstrates that in the first several months
40 following a surface spill, dilbit has a similar potential for biodegradation by a native shallow
41 subsurface microbial community as conventional heavy crude oil.

42

43 **1. Introduction**

44 The oil sands deposit in Alberta, Canada, is the world's third largest proven reserve of
45 crude oil (NRCan, 2020). The oil extracted from this region is a heavily degraded, highly viscous
46 form of petroleum known as bitumen. In order to be transported via pipeline, bitumen is diluted

47 with lighter hydrocarbon fractions such as natural gas condensates and naphtha to yield a less
48 viscous blend commonly referred to as dilbit (Radović et al., 2018). Dilbit is typically
49 manufactured at a ratio of 70-80% bitumen to 20-30% diluent (Crosby et al., 2013; Spalding and
50 Hirsh, 2012). Many of the chemical and physical properties of dilbit differ from those of
51 conventional crude oils, leading to unique behavior in the environment (Dollhopf et al., 2014;
52 Radović et al., 2018). For instance, the generally higher density and viscosity of dilbit can lead to
53 more pronounced sinking in water following a spill (Radović et al., 2018; Utting et al., 2022). As
54 a result, remediation strategies that were largely developed for conventional crude oils may not
55 necessarily be applicable to dilbit spills (Davoodi et al., 2020; Dollhopf et al., 2014). With
56 increases in dilbit production and transport expected in coming years, the risks posed by inland oil
57 spills are of great concern as they have a high potential to occur near populated areas, impact
58 groundwater systems, and affect environments with a much lower capacity to dilute and disperse
59 the oil (Lee et al., 2015).

60 Biodegradation has been demonstrated to be one of the most cost-effective and least
61 disruptive strategies for containing and removing conventional crude spills from the environment
62 (Hazen et al., 2016; Mahmoudi et al., 2017; Widdel et al., 2010; Yang et al., 2016). The success
63 of this strategy is highly site specific as it depends on both environmental conditions and the
64 abundance and diversity of microbes that possess the enzymes to break down crude oil constituents
65 (Liao et al., 2015; Liu et al., 2017; Yang et al., 2016). Currently, it is unclear to what extent dilbit
66 biodegradation is comparable to that of conventional crude oil. Previous dilbit studies, the vast
67 majority of which have focused on marine and surface freshwater environments, have shown
68 breakdown of the simplest alkane fractions (Schreiber et al., 2019), while evidence for the
69 degradation of larger aromatic fractions of dilbit has been mixed (Deshpande et al., 2018; Schreiber

70 et al., 2021). In addition, most studies examining the biodegradation of dilbit have only considered
71 short-term (< 30-day) exposures (Davoodi et al., 2020; Deshpande et al., 2017; King et al., 2014;
72 Stoyanovich et al., 2019), which greatly limits our understanding of its long-term susceptibility to
73 microbial breakdown..

74 The hydrological, geochemical and microbial conditions found in the unsaturated and
75 saturated zones of soils and aquifers compared to marine and surface freshwater environments
76 imply a different behaviour and fate for dilbit following its accidental release in terrestrial
77 ecosystems. However, despite being environments frequently impacted by pipeline ruptures
78 (Owens et al., 1993; Zhao et al., 2020), the behaviour and fate of dilbit in shallow soil and
79 groundwater systems has thus far received little attention. While not dilbit, the large crude oil spill
80 that occurred near the city of Bemidji, MN, USA in August 1979 as a result of a pipeline burst
81 along a seam weld (Essaid et al., 2011) has provided a wealth of information on natural attenuation
82 processes in petroleum-contaminated aquifers. Investigations at this site over the past few decades
83 have shed insight into temporal changes in the geochemical composition (Baedecker et al., 2018;
84 Podgorski et al., 2021), microbial communities involved with *in situ* biodegradation (Beaver et al.,
85 2021; Fahrenfeld et al., 2014), and the lasting toxicological effects of a crude oil plume (McGuire
86 et al., 2018; Zemo et al., 2022). Although previous research carried out at Bemidji and other crude
87 oil-contaminated aquifers provides a valuable reference, the unique chemical and physical
88 properties of dilbit necessitates dilbit-specific controlled spill experiments to better understand its
89 compartment in the subsurface.

90 To address this research gap, we integrated molecular and isotopic approaches to
91 investigate the response of indigenous microbial communities to a long-term (104-day) exposure
92 of dilbit using large columns as analogues to the unsaturated or vadose zone of natural groundwater

93 systems. An additional treatment using conventional heavy crude oil was conducted in parallel to
94 compare the biodegradation potential of both oils under identical, controlled conditions. Rather
95 than solely monitoring changes in petroleum hydrocarbon concentrations, an approach which does
96 not unequivocally verify biodegradation, natural abundance stable carbon ($\delta^{13}\text{C}$) and radiocarbon
97 ($\Delta^{14}\text{C}$) isotope values of microbial lipids were used to provide direct evidence for *in situ* uptake of
98 petroleum carbon. Petroleum products, including dilbit, have no detectable ^{14}C ($\Delta^{14}\text{C} = -1000\text{‰}$).
99 This contrasts with surface or near-surface soil organic matter, which has a $\Delta^{14}\text{C}$ value that more
100 closely reflects the input of recently fixed carbon ($\sim 0\text{‰}$) (Ahad et al., 2010; Slater et al., 2005).
101 Thus, the more negative the $\Delta^{14}\text{C}$ value of microbial components, the greater the assimilation of
102 petroleum-derived carbon by the microbial community. Temporal changes in microbial
103 community structure and taxonomic composition were tracked using amplicon sequencing of the
104 16S rRNA to identify key dilbit-degrading taxa (Caporaso et al., 2012; Mahmoudi et al., 2013b).
105 To our knowledge, this is the first study to examine the biodegradation of dilbit in the unsaturated
106 zone following a simulated surface spill.

107

108 **2. Materials and Methods**

109 **2.1. Column construction**

110 Approximately 2000 kg of vadose zone soil ($\sim 0\text{-}20$ cm depth) was collected in July 2019
111 from the Mount St-Hilaire Nature Reserve, approximately 40 km east of Montréal, Québec,
112 Canada. This site was chosen to provide relatively pristine soil from a region where future dilbit
113 pipeline construction may be considered. The soil was immediately transported to the Laboratories
114 for Scientific and Technological Innovation in Environment (LISTE) facility at INRS in Québec
115 City, Québec, Canada, where it was sieved through a 2 cm mesh and homogenized via mechanical

116 rotation for 10 min at 25 rpm in 205 L high density polyethylene barrels. The water content
117 following homogenization was $5.38 \pm 0.02\%$. The soil was then evenly distributed between
118 columns that were composed of stainless steel (60 cm width \times 100 cm height) lined with
119 polytetrafluoroethylene (PTFE). Within each column, 312.80 ± 0.20 kg of soil (dry mass) was
120 compacted in layers of 2 cm using a jack drill and a stainless steel plate to reproduce field soil
121 density and avoid channeling in the column that would bias water infiltration behavior. Each soil
122 layer was scarified to a depth of 5 mm using a small rake before adding the next one. The average
123 soil density was 1.59 ± 0.02 kg/L and the porosity was 0.4). The total organic carbon (TOC)
124 determined using an elemental analyzer (Costech Analytical Technologies Inc., Valencia, CA) was
125 $1.7 \pm 0.6\%$. Granulometric analysis of the soil indicated $> 99\%$ sand-sized particles, 85% of which
126 were larger than 0.5 mm.

127 Seven 1 cm diameter outflow ports in the bottom of each column directed leachate water
128 into seven 1 L amber glass bottles resting below. Ports were fitted with PTFE pipefittings with
129 fiberglass wicks threaded through them. To limit evaporation, these ports were sealed to the
130 leachate collection bottles with PTFE thread tape. Wicks were in contact with the bottom layer of
131 soil in the column and, relative to the sandy soil, had a net negative capillary pressure which helped
132 to draw the leachate from the column to maintain unsaturated conditions (Everett and McMillion,
133 1985). A diagram of the column set-up is provided in the Supporting Data (Figure S1).

134

135 **2.2. Experimental conditions**

136 The columns were designed to be representative of vadose zone systems in the Greater
137 Montréal Area during spring and fall recharge. These seasons were selected as they allow for
138 plenty of groundwater infiltration without interference from the high rates of evapotranspiration

139 that occur in the summer, or from winter snow and ice cover (Lewis et al., 2009). The columns
140 were maintained in a temperature-controlled room at 10 °C. Artificial rainwater to simulate local
141 precipitation acidity (pH 4.8; Keresztesi et al., 2020; Vet et al., 2014) was prepared using a 3:2
142 (vol/vol) stock solution of sulfuric:nitric acid and added to each column twice a week for a total
143 of 6.25 L of water per week. Measurements of dissolved oxygen in the column leachate indicated
144 aerobic conditions were maintained in all the columns over the course of the experiment.

145 Following several column waterings over a period of four days to achieve steady-state flow
146 conditions, conventional heavy crude oil and dilbit were added to the surface of the columns on
147 Day 0. The conventional heavy crude (CC) column received 1.86 kg of conventional heavy crude
148 oil, while the dilbit (DB) column received 1.89 kg of Cold Lake Blend (CLB). These amounts
149 were intended to simulate a medium-scale incident, which ramped up to an area covering 0.25
150 hectares (2500 m²) would correspond to an oil spill of approximately 20,000 L. Both samples
151 originated from transmission pipelines: CLB refers to bitumen produced by *in situ* extraction in
152 the Cold Lake region of Alberta, while the conventional heavy crude refers to various Western
153 Canada Sedimentary Basin crude oils with similar physical and chemical properties. The
154 proportions of saturates, aromatics, resins, and asphaltenes in the oils determined gravimetrically
155 following silica gel chromatography were 25.4, 51.9, 9.5, and 13.2% and 30.4, 45.8, 8.5, and
156 14.2% in the DB and CC samples, respectively. A third column was left unamended to serve as a
157 control. The experiment was carried out for a total of 104 days.

158

159 **2.3. Soil sample collection**

160 Soil cores were collected from the columns using a stainless-steel soil core sampler (AMS,
161 American Falls, ID, USA) affixed with a slide hammer and a removable 15.2 cm (length) x 3.8 cm

162 (diameter) aluminum cylinder. The core sampler and removable cylinder were rinsed with acetone
163 and distilled water between columns. The first core series was collected immediately prior to the
164 addition of the crude oil treatments to characterize the initial soil conditions on what is referred to
165 as Day 0. Coring was done on a weekly basis for the first month (Day 0, Day 6, Day 13, and Day
166 20) and then on a biweekly basis for the remainder of the experiment (Day 34, Day 48, Day 62,
167 Day 76, Day 90, and Day 104) with 10 cores collected in total. A higher frequency of coring was
168 carried out in the first month to coincide with anticipated faster column breakthrough curves for
169 more water-soluble petroleum components such as BTEX (benzene, toluene, ethylbenzene and
170 xylenes). A diagram showing the spatial arrangement of core extractions within the column set-up
171 and further details on coring protocol are provided in the Supporting Data (Figure S2, Text S1).

172 To minimize the hydraulic disturbance caused by repeated coring, core holes were filled in
173 with a 1:1 mixture of sodium bentonite clay tablets (Volclay® PureGold™ 3/8 inch, CETCO,
174 Bethlehem, PA, USA) and sodium bentonite powder (Envrioplug Grout, Wyo-Ben Inc., Billings,
175 USA) immediately following the collection of each core. This material expanded when mixed with
176 water so that the surrounding soil remained compact while still allowing water to permeate
177 vertically. The downward vertical flow of water (Figure S1), in conjunction with a sampling
178 strategy in which cores were taken at opposite sides of the column from the previous collection
179 (Figure S2), would have limited the potential impact of coring on microbial and geochemical
180 dynamics in non-cored sections of the columns.

181

182 **2.4. Total petroleum hydrocarbons (TPHs)**

183 Total Petroleum Hydrocarbons (TPHs) from soil cores were extracted and analyzed
184 following protocols similar to those described by (Ahad et al., 2010). TPHs were analyzed using

185 a gas chromatograph – mass spectrometer (GC-MS; Agilent Technologies Inc., Santa Clara, CA,
186 USA; 7890A GC and 5975C MS detector) equipped with a Zebron (Phenomenex, Inc., Torrance,
187 CA, USA) ZB-5HT column (30 m; 0.25 mm i.d.; 0.25 μ m film) at the Delta-Lab of the Geological
188 Survey of Canada (GSC-Québec). The following GC oven temperature program was used: 70 °C
189 (2 min), 8 °C/min to 290 °C (8 min), 10 °C/min to 310 °C (10 min). TPH concentrations were
190 determined by integrating the total area of unresolved complex mixture (UCM) in total ion current
191 (TIC) mode. Further details on TPH analysis are found in the Supporting Data (Text S2).

192

193 **2.5. Microbial lipid extraction and analysis**

194 Phospholipid fatty acids (PLFAs) are essential membrane lipids of microbial cells and
195 biomarkers for the active microbial population. PLFAs were extracted from sub-samples of
196 homogenized soil cores following a modified Bligh and Dyer method (White et al., 1979)
197 employed by Ahad et al. (2018) and converted to fatty acid methyl esters (FAMES) by mild
198 alkaline methanolysis adapted from Guckert et al. (1985). Further details on the lipid extraction
199 protocol are found in the Supporting Data (Text S3).

200 FAMES were analyzed using the same GC-MS system and column described above for
201 TPH analysis. The following GC oven temperature program was used: 40 °C (1 min), 20 °C/min
202 to 130 °C, 4 °C/min to 160 °C, 8 °C/min to 300 °C (5 min) as per Ahad et al. (2018). Quantification
203 was done in TIC mode using external FAME standards (12:0, 14:0, 16:0, 18:0, and 20:0).
204 Calibration curves and quantitation methods were set up using MSD ChemStation Data Analysis
205 software (Agilent). The distributions of individual PLFAs in each sample are reported here as a
206 mole percentage (mol %) relative abundance. PLFAs were identified by comparing the mass

207 fragmentation patterns and retention time to a bacterial reference standard (Bacterial Acid Methyl
208 Esters CP Mix, Sigma-Aldrich, Oakville, ON, Canada).

209 PLFAs were described as Z:n Δ x, where Z is the total number of carbon atoms on the fatty
210 acid chain, n is the number of double bonds and Δ x indicates the location of the double bond if
211 known. The letters A, B, and C denote different isomers whose double bond position is unknown.
212 Cyclopropyl PLFAs are denoted with the prefix “cyc”. Methyl group branching is denoted by the
213 prefixes “i” for the iso-isomer, “a” for the anteiso-isomer, and “br” if the position of the methyl
214 group is unknown (branched isomers are differentiated by letters A, B, and C).

215

216 **2.6. $\delta^{13}\text{C}$ analysis**

217 The stable carbon isotope contents ($\delta^{13}\text{C}$) of individual PLFAs were determined using a
218 gas chromatograph – isotope ratio mass spectrometer (GC-IRMS) at the GSC-Québec’s Delta-
219 Lab. The system consisted of a TRACE 1310 GC with a HP-5 column (60 m; 0.32 mm i.d.; 0.25
220 μm film) paired with a Delta V IRMS via a GC IsoLink (Thermo Fisher Scientific, Bremen,
221 Germany). The IsoLink combustion reactor was maintained at 1050 °C. The GC oven temperature
222 program was the same as that used for GC-MS analysis.

223 An external standard mixture containing 5- α -androstane obtained from the
224 Biogeochemical Laboratories at Indiana University and five in-house FAME isotopic standards
225 (12:0, 14:0, 16:0, 18:0, and 20:0) was injected into the GC-IRMS after every six sample injections
226 to assess accuracy. Samples were run in duplicate, and peaks were manually integrated using
227 Isodat software (Thermo Fisher Scientific) to obtain $\delta^{13}\text{C}$ ratios for specific PLFAs. The precision
228 (1σ) for replicate standard and sample injections was $\pm 0.5\%$. All $\delta^{13}\text{C}_{\text{PLFA}}$ values were corrected

229 for the isotopically characterized methyl group added to each FAME during mild alkaline
230 methanolysis by the following equation:

231

$$232 \quad \delta^{13}\text{C}_{\text{PLFA}} = [\delta^{13}\text{C}_{\text{measured}} - (f_{\text{MeOH}} \times \delta^{13}\text{C}_{\text{MeOH}})] / (1 - f_{\text{MeOH}}) \quad (1)$$

233

234 where f_{MeOH} is the fraction of C atoms derived from methanol (MeOH). The $\delta^{13}\text{C}_{\text{MeOH}}$ value was -
235 51.3‰.

236 The $\delta^{13}\text{C}$ values of total organic carbon (TOC) in decarbonated soil samples were measured
237 using an elemental analyser (Costech Analytical Technologies Inc.) interfaced with a Delta V
238 (Thermo Fisher Scientific) IRMS system. Further details on sample preparation are provided in
239 the Supporting Information (Text S4).

240

241 **2.7. $\Delta^{14}\text{C}$ analysis**

242 The masses of individual PLFAs were too low for compound-specific radiocarbon analysis;
243 consequently, ^{14}C contents were determined in the bulk PLFA fractions (Ahad et al., 2010;
244 Mahmoudi et al., 2013a). In some cases, samples from multiple depths were combined to meet
245 mass requirements for bulk ^{14}C analyses. Samples for radiocarbon analysis were selected at four
246 different time series covering the full length of the experiment.

247 FAMES dissolved in dichloromethane (DCM) were transferred by syringe into a 40 μL
248 rigid silver capsule (IVA-Analysentechnik e.K.), dried in an oven at 50 °C for 30 min, and sealed
249 with pliers following a protocol similar to that previously used for preparation of organic extracts
250 for ^{14}C analysis (Ahad et al., 2020; Ahad et al., 2021). Samples were placed in quartz tubes with
251 CuO oxidizer, sealed under vacuum, and combusted to CO_2 at 900 °C. CO_2 was then reduced to

252 graphite and measured for its $^{14}\text{C}/^{12}\text{C}$ ratio using a 500 kV compact accelerator mass spectrometer
 253 (AMS) unit (National Electrostatics Corporation, Middleton, WI, USA) at the W.M. Keck Carbon
 254 Cycle AMS facility at the University of California Irvine. Ratios were then corrected with the ratio
 255 of Oxalic Acid I (SRM 4990) and normalized for ^{13}C fractionation to be presented in the standard
 256 $\Delta^{14}\text{C}$ notation (Stuiver and Polach, 1977).

257 The radiocarbon contents of total organic carbon (TOC) in freeze-dried soil samples (also
 258 reported in $\Delta^{14}\text{C}$ notation) were determined using the same AMS system described above. TOC
 259 samples were decarbonated with 1N HCl at 70 °C, washed with ultrapure MilliQ water and dried
 260 prior to combustion to CO_2 .

261 To assess the accuracy and precision of $\Delta^{14}\text{C}$ analyses, both modern (butter-derived
 262 FAMEs) and fossil (Ordovician shale aromatic hydrocarbons) standards of similar masses to those
 263 of samples were prepared in the same manner as described above. Based on replicate analyses of
 264 these standards, the error incorporating both accuracy and precision for $\Delta^{14}\text{C}$ analyses was < 20%.
 265 All $\Delta^{14}\text{C}_{\text{PLFA}}$ values were corrected for the isotopically characterized methyl group added to each
 266 FAME during mild alkaline methanolysis by the following equation:

$$267 \Delta^{14}\text{C}_{\text{MeOH}} = [\Delta^{14}\text{C}_{\text{measured}} - (f_{\text{MeOH}} \times \Delta^{14}\text{C}_{\text{MeOH}})] / (1 - f_{\text{MeOH}}) \quad (2)$$

269 where f is the fraction of C atoms derived from MeOH on each FAME. The $\Delta^{14}\text{C}_{\text{MeOH}}$ value was -
 270 998.2‰. Contributions of potential carbon sources to ^{14}C content of bulk PLFA fractions were
 271 estimated using a two end-member mass balance:
 272

$$273 \Delta^{14}\text{C}_{\text{PLFA}} = (1 - f_{\text{soil}}) \times \Delta^{14}\text{C}_{\text{petroleum}} + f_{\text{soil}} \times \Delta^{14}\text{C}_{\text{soil}} \quad (3)$$

275
276 where $\Delta^{14}\text{C}_{\text{PLFA}}$ corresponds to the isotopic value of the PLFAs, f_{soil} is the fraction of carbon
277 contributed by the background soil TOC, $1 - f_{\text{soil}}$ is the fraction of carbon contributed by petroleum,
278 $\Delta^{14}\text{C}_{\text{petroleum}}$ is the isotopic value of DB or CC (both assumed to be -1000‰) and $\Delta^{14}\text{C}_{\text{soil}}$ is the
279 isotopic value of the background soil TOC.

280

281 **2.8. Genomic DNA extraction and sequencing of 16S rRNA genes**

282 Genomic DNA was extracted from 45 soil cores, in replicate, using the DNeasy PowerSoil
283 DNA extraction kit from Qiagen (Hilden, Germany) following the manufacturer's protocol. The
284 V4 hypervariable region of the 16S rRNA gene in both bacteria and archaea (primer pair 548F and
285 806R) (Kozich et al., 2013) was amplified and sequenced in duplicate for each soil core.
286 Amplicons were sequenced on an Illumina MiSeq (San Diego, CA, USA) in the Ronholm Lab
287 (McGill University). Sequence data was analyzed using Quantitative Insights Into Microbial
288 Ecology 2 (QIIME2) v2021.2 (Bolyen et al., 2019). Files generated in the QIIME2 pipeline were
289 then exported for use in downstream statistical analyses. Details of sequence data processing using
290 QIIME2 can be found in the Supporting Information (Text S5). Sequencing data were submitted
291 to the National Center for Biotechnology Information (NCBI) under BioProject PRJNA922993.

292

293 **2.9. Statistical analyses of sequencing data**

294 All statistical analyses and visualizations were done in R, version 4.0.2. Amplicon
295 sequence variant (ASV) counts were rarefied (subsampling without replacement) to 4162, which
296 equated to the sample with the lowest number of reads, using the phyloseq R package (McMurdie
297 and Holmes, 2013). Beta diversity metrics were calculated using Weighted UniFrac distance with

298 phyloseq. Results of the distance matrix were visualized by Principal Coordinate Analysis (PCoA)
299 using the phyloseq and ggplot2 R packages (Wickham, 2011). Differences in microbial community
300 composition between metadata groups (treatment type/sample depth/sample day) were assessed
301 using permutational multivariate analysis of variance (PERMANOVA). The homogeneity of
302 within-group dispersions was assessed by permutation multivariate analysis of dispersion
303 (PERMDISP). Both PERMANOVA and PERMDISP were implemented using the vegan R
304 package (Oksanen et al., 2013).

305 Normality and homogeneity of variance of the relative abundance of individual taxonomic
306 groups were evaluated with the Shapiro-Wilk test ($P < 0.05$) and the Levene's test ($P < 0.05$),
307 respectively. For all datasets, the assumptions of normality and equal variance required for analysis
308 of variance (ANOVA) tests were not met. As an alternative to ANOVA, the non-parametric
309 Kruskal-Wallis test followed by a Dunn's multiple comparison test with Holm adjustment was
310 done to reveal if significant differences existed between metadata groups (treatment type/sample
311 depth/sample day) in these datasets. These calculations were done using the rstatix package
312 (Kassambara, 2021).

313

314 **3. Results**

315 **3.1. Concentrations of TPHs**

316 Concentrations of TPHs extracted from soil cores ranged from 19 to 568 mg/kg in DB,
317 19.5 to 605 mg/kg in CC, and 24 to 27.6 mg/kg in the control (Table S2). TPH concentrations were
318 highest in the top depths of DB and CC cores (404 to 605 mg/kg) and were comparable to the
319 lower range of those reported in soils contaminated by crude oil near pipelines (Iturbe et al., 2007;
320 Pernar et al., 2006). TPH concentrations at middle and bottom depths remained at similar levels to

321 the control over the course of the experiment apart from the bottom depth of DB, which spiked to
322 91 mg/kg on Day 34. The background TPH concentration in the control (24.0 to 27.6 mg/kg) is
323 attributed to the presence of non-petroleum hydrocarbons (e.g., alkanes from plant leaf waxes)
324 found in the soil.

325

326 **3.2. Microbial PLFAs**

327 The total concentrations of PLFAs extracted from individual samples varied widely over
328 the course of the exposure but did not show any trends across metadata groups (treatment type,
329 sample depth, sample day). Total PLFA concentrations ranged from 8.18 to 37.57 ng/g soil, with
330 much of this variability likely attributable to differences in grain size from sample to sample
331 (Figure S3). Overall, PLFA distributions (as mol %) for the most abundant compounds were
332 similar across all samples (Figure 1). The most abundant PLFAs across all DB, CC, and control
333 samples were 16:0 (17.0 to 23.0%) and 18:1B (10.4 to 16.2%). In all columns, 16:0, a general
334 bacterial biomarker, and 18:1B, a biomarker for gram-negative bacteria (Wilkinson and Ratledge,
335 1988), showed a slight increase in abundance over the exposure period. The gram-positive
336 bacterial biomarkers, i-15:0 and a-15:0 (O'Leary et al., 1988; Vestal and White, 1989) both
337 decreased for DB and CC columns. In contrast, cyc17:0, a biomarker for gram-negative bacteria
338 and petroleum-degrading bacteria (Ahad et al., 2018; Cowie et al., 2010; Greenwood et al., 2009),
339 only increased in CC and DB columns (Figure 1).

340 Principle Component Analysis (PCA) was performed on mol % data for the top 12 PLFAs
341 from each depth separately (Text S6). PCA biplots showed a progressive change in PLFA
342 distributions over time in oil-impacted samples and the control (Figure S4). Greater mol % of
343 cyc17:0, 16:0, 16:1 Δ 9, and 18:1B were associated with CC and DB samples in the later stages of

344 the exposure period (after day 48). All other PLFAs were associated with control and early-stage
345 (before day 48) DB and CC samples. The PCA biplots indicate changes in microbial PLFA
346 distributions in response to oil exposure but no distinction between DB- and CC-impacted
347 communities.

348

349 3.3. $\delta^{13}\text{C}$ values of PLFAs and TOC

350 The $\delta^{13}\text{C}$ values of individual PLFAs ranged from -30.5 to -24.0‰ (Figure 2). In general,
351 the $\delta^{13}\text{C}$ values of individual PLFAs showed no clear trends across depths or time. The $\delta^{13}\text{C}$ -PLFA
352 values have thus been grouped to highlight potential differences between treatments (Figure 2).
353 The most enriched PLFA was a-15:0, with an average $\delta^{13}\text{C}$ value from all three columns (DB, CC,
354 and control) of $-25.2 \pm 0.5\%$ over the entire length of the experiment. The most depleted PLFA
355 was 19:1A, with an average $\delta^{13}\text{C}$ value of $-29.0 \pm 0.7\%$.

356 There were statistically significant differences in $\delta^{13}\text{C}$ values for cyc17:0 ($P < 0.05$) and
357 the combined PLFAs 16:1 Δ 9 and 16:1B ($P < 0.05$) between the control and both oil-impacted
358 columns. The $\delta^{13}\text{C}$ values of cyc17:0 were significantly more depleted in both CC and DB
359 compared to the control ($P < 0.05$). The combined 16:1 Δ 9 and 16:1B group was significantly more
360 depleted in ^{13}C in CC compared to the control ($P < 0.05$).

361 The $\delta^{13}\text{C}$ values of the control soil TOC on Day 0 were -26.8, -27.6 and -27.4‰ in the top,
362 middle and bottom core sections, respectively, and remained unchanged over the course of the
363 experiment ($-27.2 \pm 0.1\%$ on Day 104). On Day 6, the $\delta^{13}\text{C}$ -TOC values in the in the top, middle
364 and bottom core sections of the DB and CC columns were -29.0, -27.5 and -27.7‰ and -29.2, -
365 27.9 and -27.2‰, respectively. The more depleted values in the top sections reflected a greater
366 contribution from either dilbit (-29.9‰) or conventional heavy crude (-29.3‰). This trend

367 remained consistent over the course of the experiment, as evident from a similar suite of values
368 measured in top, middle and bottom core sections on Day 104 (DB: -29.3, -27.3 and -26.8‰; CC:
369 -29.1, -27.4 and -27.4‰).

370

371 **3.4. $\Delta^{14}\text{C}$ values of bulk PLFAs**

372 Bulk PLFA ^{14}C contents for DB and CC columns were assessed from individual top,
373 middle and bottom depths on Days 34 and 62 and from combined depths on Day 104 (Table S3,
374 Figure 3). Bulk PLFA ^{14}C contents in the control were determined from individual top, middle and
375 bottom depths on Days 34 and 62 and from combined depths on Days 0 and 104 (Table S3, Figure
376 3). The $\Delta^{14}\text{C}$ values of bulk PLFAs in the control ranged from -46.1 to +53.7‰ and for most
377 samples were more positive than the $\Delta^{14}\text{C}$ value of the bulk soil TOC (-34.7‰). The $\Delta^{14}\text{C}$ values
378 of bulk PLFAs ranged from -221.1 to -54.7‰ in the DB column and from -259.4 to -97.9‰ in the
379 CC column. In contrast to the control, there was a discernible decrease in $\Delta^{14}\text{C}$ values for both CC
380 and DB columns over the exposure period (Figure 3).

381

382 **3.5. Microbial community composition**

383 Sequencing of 16S amplicons yielded a total of 6,382,607 reads. Following quality control,
384 the total read count was reduced to 3,812,693 with an average of 39,715 reads per sample. The
385 total number of amplicon sequence variants (ASVs) present in the filtered dataset was 26,641. The
386 overwhelming majority of ASVs (17,736) were assigned to *Bacteria* and only 69 were assigned to
387 *Archaea*. The dominant bacterial phylum across all samples was *Proteobacteria*, making up 32.7
388 to 60.1% of ASVs across all samples (Figure S5). Other abundant phyla (> 1% average abundance)
389 included *Actinobacteriota* (8.5 to 21.4%), *Acidobacteriota* (6.8 to 17.0%), *Chloroflexi* (2.6 to

390 9.7%), *Bacteroidota* (1.7 to 19.8%), *Myxococcota* (0.8 to 7.8%), *Verrucomicrobiota* (1.2 to 6.9%),
391 *Planctomycetota* (0.8 to 5.9%), *Gemmatimonadota* (1.3 to 3.7%), and *Firmicutes* (0.4 to 6.0%).
392 *Gammaproteobacteria* was the dominant class (Figure S6) across all samples. There were
393 significant differences in the relative abundance of *Gammaproteobacteria* between control and
394 oil-impacted columns ($P < 0.05$). During the exposure period, the average relative abundance of
395 *Gammaproteobacteria* increased by 11.7 and 16.1% in the DB and CC columns, respectively. In
396 contrast, the average relative abundance of *Gammaproteobacteria* remained at 19.4% in the
397 control column. Within *Gammaproteobacteria*, the predominant order was *Burkholderiales*
398 (Figure S7) whose relative abundance significantly increased by 11.5% and 15.3% in both the DB
399 and CC columns ($P < 0.05$). At the genus level, dramatic increases in relative abundances of
400 *Polaromonas* from within the order *Burkholderiales* were observed over time (Figure 4). At day
401 0, *Polaromonas* accounted for $< 1\%$ of sequences but by day 104 it comprised 8.9 to 18.2% of all
402 sequences in the DB samples (across all depths) and 8.0 to 17.2% in the CC samples (across all
403 depths) while accounting for $< 1\%$ of sequences in the control column.

404 Several other groups became more abundant in the oil-impacted columns compared to the
405 control column over time (Figure 4). There were significantly higher proportions of
406 *Phenylobacterium* (*Alphaproteobacteria*), *Mycobacterium* (*Actinobacteria*), and an unknown
407 genus from the family *Comamonadaceae* (the same family as *Polaromonas*) in both the DB and
408 CC samples relative to the control ($P < 0.05$).

409 Changes in microbial community structure over time were visualized for each sampling
410 depth (top, middle and bottom) using PCoA of weighted unifracs distances based on the relative
411 abundance of ASVs (Figure S8). For all three depths, the DB and CC samples were significantly
412 different from the control samples ($P < 0.05$) but not from each other. This implies that although

413 microbial communities were strongly affected by the presence of oil, the type of oil (DB vs. CC)
414 did not lead to specific changes in community composition. Likewise, PERMANOVA tests found
415 no significant differences between the microbial communities exposed to DB and CC but did
416 clearly differentiate them from Day 0 and control samples ($P < 0.05$).

417

418 **4. Discussion**

419 Although subtle (Figure 1), the distributions of PLFAs in DB, CC, and control columns
420 changed over the course of the experiment. The increases in the mol % of cyc17:0, 16:0, 18:1B
421 and 16:1 Δ 9 and decreases in a-15:0, and i-15:0 were associated with microbial communities
422 exposed to CC and DB. Cyc17:0, 18:1B, and 16:1 Δ 9 are biomarkers for gram-negative bacteria
423 (Wilkinson and Ratledge, 1988). Previous studies have reported similar increases in the abundance
424 of gram-negative PLFA biomarkers following exposure to petroleum (Bastida et al., 2016; Green
425 and Scow, 2000; Li et al., 2018; Margesin et al., 2007). In addition to being a biomarker for gram-
426 negative bacteria, cyc17:0 has been associated with petroleum-degrading microbes in previous
427 studies (Ahad et al., 2018; Cowie et al., 2010; Greenwood et al., 2009). Correspondingly, this
428 increase in gram-negative was confirmed by the amplicon sequencing data which revealed that the
429 gram-negative bacterial phylum, *Proteobacteria*, dominated the microbial community and their
430 relative abundances increased over the exposure period in DB and CC columns.

431 *Proteobacteria* are known to include a multitude of hydrocarbon-degrading bacteria that
432 contribute to crude oil degradation (Ahad et al., 2018; Bastida et al., 2016; Deshpande et al., 2018;
433 Hazen et al., 2016; Mahmoudi et al., 2013b). The dominant DB and CC-degrader identified in our
434 study was *Polaromonas*, a genus within the order *Burkholderiales*. In addition to *Polaromonas*,
435 several other genera significantly increased in abundance during the DB and CC exposures. These

436 included *Phenylobacterium*, *Mycobacterium*, and an unknown genus from the family
437 *Comamonadaceae* – all of which are known oil-degrading bacteria (Atlas et al., 2015; Kweon et
438 al., 2011; Rodgers-Vieira et al., 2015; Yang et al., 2016). Previous genomic analyses have shown
439 that numerous bacteria within the taxa *Burkholderiales*, including *Polaromonas*, have the
440 metabolic potential to degrade a broad spectrum of aromatics as they possesses genes used in many
441 peripheral and central ring-cleavage pathways (Hanson et al., 2012; Jeon et al., 2003; Pérez-
442 Pantoja et al., 2012). Moreover, *Polaromonas* spp. were identified as potential dilbit-degraders in
443 a recent study monitoring biodegradation of two types of dilbit (CLB and Western Canadian
444 Select) by bacterial enrichments in freshwater microcosms (Deshpande et al., 2018). In their 72-
445 day experiment using an enriched microbial consortium obtained from sediment contaminated by
446 the 2010 Kalamazoo River dilbit spill, Deshpande et al. (2018) noted that relative abundance of
447 *Polaromonas* and other bacterial genera increased as concentrations of larger aromatic and
448 branched alkane fractions decreased. *Polaromonas* reached its highest abundance on day 40 for
449 CLB and day 72 for Western Canadian Select dilbit. In our study, *Polaromonas* reached its highest
450 relative abundance more than three months following the spill, on Day 104. This slow but
451 consistent increase suggests *Polaromonas* was potentially metabolizing the larger, more complex
452 hydrocarbon fractions that did not undergo immediate weathering.

453 Hydrocarbon metabolism by bacteria under aerobic conditions results in $\delta^{13}\text{C}$ -PLFA values
454 that closely mirror that of the carbon source (typically PLFAs are depleted by $< 3\text{‰}$) (Ahad and
455 Pakdel, 2013; Cowie et al., 2010; Hayes, 2001). The observation that all $\delta^{13}\text{C}$ PLFA values were
456 within 3‰ of the potential carbon sources thus reflects the oxic conditions in soil columns and
457 aerobic biodegradation of DB and CC (Figure 2). The depleted $\delta^{13}\text{C}$ values for cyc17:0 and the
458 combined 16:1 Δ 9 and 16:1B in DB and CC relative to the control pointed to uptake of ^{13}C -depleted

459 oil (DB: -29.9‰; CC: -29.3‰) relative to more ^{13}C -enriched soil TOC (-27.3‰). Both PLFAs are
460 biomarkers for gram-negative bacteria and were previously observed to be associated with oil-
461 degrading microbial communities (Ahad et al., 2018; Greenwood et al., 2009). Interestingly,
462 *Polaromonas* strains have been shown to predominantly feature 16:1 Δ 9 and cyc17:0 in their PLFA
463 profiles (Kämpfer et al., 2006; Sizova and Panikov, 2007). The more positive $\delta^{13}\text{C}$ values for i-
464 15:0 and a-15:0 show the carbon source to be background soil TOC rather than the ^{13}C -depleted
465 oil. The growth of the subset of soil microbes preferring soil organic matter was not promoted by
466 the presence of DB or CC, and as such the relative abundances of i-15:0 and a-15:0 decreased as
467 PLFAs associated with oil degradation (e.g., cyc17:0) increased (Figure 1). There were no
468 discernable trends in $\delta^{13}\text{C}$ values over time or between depths, likely due to the small differences
469 between the $\delta^{13}\text{C}$ of TOC and the two oils (2.0 and 2.6‰ for DB and CC, respectively), relative to
470 the margin of error in $\delta^{13}\text{C}$ measurements ($\pm 0.5\text{‰}$).

471 Sorption onto organic matter and heterogeneous distributions between samples make
472 determining mass losses of TPHs in soils and sediments difficult to quantify (Ahad et al., 2010;
473 Slater et al., 2005). In the shallow subsurface, dispersion and advection play important roles in
474 controlling contaminant concentrations over time (Kalbe et al., 2008). As shown on Table S2, there
475 were no consistent changes in TPH concentrations in the top, middle and bottom core sections
476 over the course of this experiment. In contrast, the significant differences in $\Delta^{14}\text{C}$ -PLFA values
477 between DB/CC and control columns on Days 34, 62, and 104 (Figure 3) provided unequivocal
478 evidence for microbial uptake of petroleum-derived carbon throughout the exposure period.
479 Although TPH concentrations showed no clear temporal trends, in general the $\Delta^{14}\text{C}$ values of bulk
480 PLFAs reflected the level of petroleum contamination in the soil. For example, higher

481 concentrations of TPHs in the top depths of DB and CC cores corresponded to lower $\Delta^{14}\text{C}$ -PLFA
482 values that indicated greater levels of microbial uptake of oil (Tables S2 and S3).

483 Using the two end-member mass balance (Eq. 3), we calculated the relative contribution
484 of carbon sources to the ^{14}C contents of the PLFAs in the DB and CC samples (Table S3). Between
485 2 and 19% and 7 and 23% of microbial PLFA carbon was derived from petroleum in columns
486 amended with DB and CC, respectively. Thus, while there was certainly uptake of DB and CC,
487 the background soil organic matter remained the dominant carbon source for microbial
488 communities. The slightly more positive $\Delta^{14}\text{C}$ -PLFA values in the control ($+10.7 \pm 38.6\%$)
489 compared to bulk soil TOC (-34.7%) indicated that microbes were preferentially degrading the
490 more modern (i.e., more recently fixed from atmospheric CO_2) and ostensibly labile constituents
491 within the background soil TOC, a finding observed in previous studies (Cowie et al., 2010;
492 Kramer and Gleixner, 2008).

493 The preferential uptake of more modern background soil TOC at petroleum-contaminated
494 sites has been observed in other studies that determined $\Delta^{14}\text{C}$ values in bulk PLFAs. In an
495 investigation into carbon sources utilized by the active microbial communities in shallow
496 groundwater systems underlying three petroleum service stations, Ahad et al. (2010) found that
497 higher petroleum concentrations and lower soil TOC levels corresponded to greater utilization of
498 fossil carbon (up to 43%). The preferential microbial utilization of relatively more modern carbon
499 sources was also observed in soils surrounding a former industrial site, where maximum
500 contributions of fossil PAH-derived carbon in microbial PLFAs were found to range from 12 to
501 71% (Mahmoudi et al., 2013a). In Athabasca oil sands region tailings ponds – systems dominated
502 by fossil carbon sources – Ahad and Pakdel (2013) reported $\Delta^{14}\text{C}$ values of up to around -600%
503 for non-specific PLFAs (e.g., 16:0). Dissolved and particulate organic matter from the Athabasca

504 River, the main source of freshwater used by bitumen mining companies, was considered the main
505 source for the relatively modern carbon preferred by tailings sediment microbes.

506 The $\Delta^{14}\text{C}$ values of bulk PLFAs in the control at middle, bottom and combined depths
507 ranged from +0.3 to +53.7‰. However, the $\Delta^{14}\text{C}$ values in the top depths of the control were
508 significantly more negative with Day 34 and Day 62 values at -28.5 and -46.1‰, respectively
509 (Figure 3, Table S3). This discrepancy can be attributed to the release of volatile organic
510 compounds from neighbouring DB and CC columns contaminating the top depth of the control,
511 leading to potential uptake of ^{14}C -depleted hydrocarbons by control column microbes. This theory
512 is supported by the trends in amplicon sequencing results. During the exposure period, microbial
513 community composition in the top depth of the control was significantly different than in middle
514 and bottom depths ($P < 0.05$). In addition, the microbial community in the control on Day 0 was
515 significantly different from all other days of the exposure ($P < 0.05$).

516

517 **5. Conclusions**

518 The production and transportation of dilbit is expected to increase in coming decades
519 (CAPP, 2019), leading to a greater risk for accidental release into the environment. Understanding
520 the behaviour of dilbit in the shallow subsurface following a spill is a key component of responsible
521 resource development. Over a 104-day exposure period using large-scale columns, we observed
522 direct evidence of continuous microbial uptake of dilbit in simulated vadose zone systems.
523 Similarities in the microbial response to DB and CC spills demonstrated that, under aerobic
524 conditions, the biodegradation potential of these two oils in the shallow subsurface is equal.

525 The experiments reported here were carried out using a sandy soil with a TOC content of
526 $1.7 \pm 0.6\%$. Variations in these and other soil parameters (e.g., microbial community composition,

527 moisture level, etc.) may have led to different levels of natural attenuation in both DB and CC
528 columns. A goal of future work should thus be to examine the shallow subsurface behaviour of
529 DB under a variety of different experimental conditions. Data generated by this study and
530 additional controlled spill experiments can be used to inform the development of effective DB spill
531 response strategies, specifically the potential for biodegradation by natural soil microbial
532 communities in the unsaturated zone to act as a remediation strategy.

533

534 **Acknowledgements**

535 We thank Marc Luzincourt, Anna Smirnoff, Hooshang Pakdel and Jade Bergeron (Delta-
536 Lab, GSC-Québec) for help with sample preparation and laboratory analyses, Nicholas Gibb
537 (GSC-Québec) for help with soil collection, Patrick Watt (Delta-Lab, GSC-Québec) and Luc
538 Trépanier and Marie-Pierre Trépanier (INRS) for assistance with column set-up. We also wish to
539 thank the Canadian Association of Petroleum Producers (CAPP) for providing us with dilbit and
540 conventional heavy crude samples, the McGill Gault Nature Reserve for providing the soil, the
541 Ronholm Lab (McGill University) for performing the DNA sequencing and the W.M. Keck
542 Carbon Cycle AMS facility (University of California Irvine) for carrying out radiocarbon analyses.
543 This research was funded by Natural Resources Canada's (NRCan's) Environmental Geoscience
544 Program through the "Environmental impact of diluted bitumen" project. This is NRCan
545 contribution number 20220083.

546

547 **Appendix A. Supplementary data**

548 The following is the Supplementary data to this article:

549

550 **References**

- 551
552 Ahad, J.M.E., Burns, L., Mancini, S., Slater, G.F., 2010. Assessing Microbial Uptake of
553 Petroleum Hydrocarbons in Groundwater Systems Using Natural Abundance Radiocarbon.
554 *Environmental Science & Technology* 44, 5092-5097.
- 555 Ahad, J.M.E., Pakdel, H., 2013. Direct evaluation of in situ biodegradation in Athabasca oil
556 sands tailings ponds using natural abundance radiocarbon. *Environmental Science & Technology*
557 47, 10214–10222.
- 558 Ahad, J.M.E., Pakdel, H., Gammon, P.R., Mayer, B., Savard, M.M., Peru, K.M., Headley, J.V.,
559 2020. Distinguishing Natural from Anthropogenic Sources of Acid Extractable Organics in
560 Groundwater near Oil Sands Tailings Ponds. *Environmental Science & Technology* 54, 2790-
561 2799.
- 562 Ahad, J.M.E., Pakdel, H., Gammon, P.R., Siddique, T., Kuznetsova, A., Savard, M.M., 2018.
563 Evaluating in situ biodegradation of ¹³C-labelled naphthenic acids in groundwater near oil sands
564 tailings ponds. *Science of the Total Environment* 643, 392-399.
- 565 Ahad, J.M.E., Pakdel, H., Labarre, T., Cooke, C.A., Gammon, P.R., Savard, M.M., 2021.
566 Isotopic Analyses Fingerprint Sources of Polycyclic Aromatic Compound-Bearing Dust in
567 Athabasca Oil Sands Region Snowpack. *Environmental Science & Technology* 55, 5887-5897.
- 568 Atlas, R.M., Stoeckel, D.M., Faith, S.A., Minard-Smith, A., Thorn, J.R., Benotti, M.J., 2015. Oil
569 biodegradation and oil-degrading microbial populations in marsh sediments impacted by oil from
570 the Deepwater Horizon well blowout. *Environmental Science & Technology* 49, 8356-8366.
- 571 Baedeker, M.J., Eganhouse, R.P., Qi, H., Cozzarelli, I.M., Trost, J.J., Bekins, B.A., 2018.
572 Weathering of oil in a surficial aquifer. *Groundwater* 56, 797-809.
- 573 Bastida, F., Jehmlich, N., Lima, K., Morris, B., Richnow, H., Hernández, T., Von Bergen, M.,
574 García, C., 2016. The ecological and physiological responses of the microbial community from a
575 semiarid soil to hydrocarbon contamination and its bioremediation using compost amendment.
576 *Journal of Proteomics* 135, 162-169.
- 577 Beaver, C.L., Atekwana, E.A., Bekins, B.A., Ntarlagiannis, D., Slater, L.D., Roszbach, S., 2021.
578 Methanogens and their syntrophic partners dominate zones of enhanced magnetic susceptibility
579 at a petroleum contaminated site. *Frontiers in Earth Science* 9, 598172.
- 580 Bolyen, E., Rideout, J.R., Dillon, M.R., Bokulich, N.A., Abnet, C.C., Al-Ghalith, G.A.,
581 Alexander, H., Alm, E.J., Arumugam, M., Asnicar, F., 2019. Reproducible, interactive, scalable
582 and extensible microbiome data science using QIIME 2. *Nature biotechnology* 37, 852-857.
- 583 Caporaso, J.G., Lauber, C.L., Walters, W.A., Berg-Lyons, D., Huntley, J., Fierer, N., Owens,
584 S.M., Betley, J., Fraser, L., Bauer, M., 2012. Ultra-high-throughput microbial community
585 analysis on the Illumina HiSeq and MiSeq platforms. *The ISME journal* 6, 1621-1624.

- 586 CAPP, 2019. 2019 Crude Oil Forecast, Markets and Transportation. Canadian Association of
587 Petroleum Producers, p. 26.
- 588 Cowie, B.R., Greenberg, B.M., Slater, G.F., 2010. Determination of Microbial Carbon Sources
589 and Cycling during Remediation of Petroleum Hydrocarbon Impacted Soil Using Natural
590 Abundance ¹⁴C Analysis of PLFA. *Environmental Science & Technology* 44, 2322-2327.
- 591 Crosby, S., Fay, R., Groark, C., Kanī, ‘., Smith, J.R., Sullivan, T., Pavia, R., Shigenaka, G.,
592 2013. Transporting Alberta oil sands products : defining the issues and assessing the risks.
593 NOAA technical memorandum NOS-OR&R ; 44.
- 594 Davoodi, S.M., Miri, S., Taheran, M., Brar, S.K., Galvez-Cloutier, R., Martel, R., 2020.
595 Bioremediation of Unconventional Oil Contaminated Ecosystems under Natural and Assisted
596 Conditions: A Review. *Environmental Science & Technology* 54, 2054-2067.
- 597 Deshpande, R.S., Sundaravadivelu, D., Campo, P., SantoDomingo, J.W., Conmy, R.N., 2017.
598 Comparative study on rate of biodegradation of diluted bitumen and conventional oil in fresh
599 water, *International Oil Spill Conference Proceedings*. International Oil Spill Conference, pp.
600 2256-2267.
- 601 Deshpande, R.S., Sundaravadivelu, D., Techtmann, S., Conmy, R.N., Santo Domingo, J.W.,
602 Campo, P., 2018. Microbial degradation of Cold Lake Blend and Western Canadian select dilbits
603 by freshwater enrichments. *Journal of Hazardous Materials* 352, 111-120.
- 604 Dollhopf, R.H., Fitzpatrick, F.A., Kimble, J.W., Capone, D.M., Graan, T.P., Zelt, R.B., Johnson,
605 R., 2014. Response to heavy, non-floating oil spilled in a Great Lakes river environment: a
606 multiple-lines-of-evidence approach for submerged oil assessment and recovery, *International*
607 *Oil Spill Conference Proceedings*. American Petroleum Institute, pp. 434-448.
- 608 Essaid, H.I., Bekins, B.A., Herkelrath, W.N., Delin, G.N., 2011. Crude Oil at the Bemidji Site:
609 25 Years of Monitoring, Modeling, and Understanding. *Groundwater* 49, 706-726.
- 610 Everett, L.G., McMillion, L.G., 1985. Operational ranges for suction lysimeters. *Groundwater*
611 *Monitoring & Remediation* 5, 51-60.
- 612 Fahrenfeld, N., Cozzarelli, I.M., Bailey, Z., Pruden, A., 2014. Insights into biodegradation
613 through depth-resolved microbial community functional and structural profiling of a crude-oil
614 contaminant plume. *Microbial Ecology* 68, 453-462.
- 615 Green, C.T., Scow, K.M., 2000. Analysis of phospholipid fatty acids (PLFA) to characterize
616 microbial communities in aquifers. *Hydrogeology Journal* 8, 126-141.
- 617 Greenwood, P.F., Wibrow, S., George, S.J., Tibbett, M., 2009. Hydrocarbon biodegradation and
618 soil microbial community response to repeated oil exposure. *Organic Geochemistry* 40, 293-300.
- 619 Guckert, J.B., Antworth, C.P., Nichols, P.D., White, D.C., 1985. Phospholipid, ester-linked fatty
620 acid profiles as reproducible assay for change in prokaryotic community structure of estuarine
621 sediments. *FEMS Microbiology Ecology* 31, 147-158.

- 622 Hanson, B.T., Yagi, J.M., Jeon, C.O., Madsen, E.M., 2012. Role of nitrogen fixation in the
623 autecology of *Polaromonas naphthalenivorans* in contaminated sediments. *Environmental*
624 *Microbiology* 14, 1544-1557.
- 625 Hayes, J.M., 2001. Fractionation of carbon and hydrogen isotopes in biosynthetic processes,
626 *Stable Isotope Geochemistry*. Mineralogical Soc America, Washington, pp. 225-277.
- 627 Hazen, T.C., Prince, R.C., Mahmoudi, N., 2016. Marine Oil Biodegradation. *Environmental*
628 *Science & Technology* 50, 2121-2129.
- 629 Iturbe, R., Flores, C., Castro, A., Torres, L.G., 2007. Sub-soil contamination due to oil spills in
630 six oil-pipeline pumping stations in northern Mexico. *Chemosphere* 68, 893-906.
- 631 Jeon, C., Park, W., Padmanabhan, P., DeRito, C., Snape, J., Madsen, E., 2003. Discovery of a
632 bacterium, with distinctive dioxygenase, that is responsible for in situ biodegradation in
633 contaminated sediment. *Proceedings of the National Academy of Sciences* 100, 13591-13596.
- 634 Kalbe, U., Berger, W., Eckardt, J., Simon, F.-G., 2008. Evaluation of leaching and extraction
635 procedures for soil and waste. *Waste management* 28, 1027-1038.
- 636 Kämpfer, P., Busse, H.-J., Falsen, E., 2006. *Polaromonas aquatica* sp. nov., isolated from tap
637 water. *International journal of systematic and evolutionary microbiology* 56, 605-608.
- 638 Kassambara, A., 2021. Pipe-friendly framework for basic statistical tests, R Package Rstatix,
639 Version 0.7.0.
- 640 Keresztesi, Á., Nita, I.-A., Boga, R., Birsan, M.-V., Bodor, Z., Szép, R., 2020. Spatial and long-
641 term analysis of rainwater chemistry over the conterminous United States. *Environmental*
642 *Research* 188, 109872.
- 643 King, T.L., Robinson, B., Boufadel, M., Lee, K., 2014. Flume tank studies to elucidate the fate
644 and behavior of diluted bitumen spilled at sea. *Marine Pollution Bulletin* 83, 32-37.
- 645 Kozich, J.J., Westcott, S.L., Baxter, N.T., Highlander, S.K., Schloss, P.D., 2013. Development of
646 a dual-index sequencing strategy and curation pipeline for analyzing amplicon sequence data on
647 the MiSeq Illumina sequencing platform. *Applied and Environmental Microbiology* 79, 5112-
648 5120.
- 649 Kramer, C., Gleixner, G., 2008. Soil organic matter in soil depth profiles: distinct carbon
650 preferences of microbial groups during carbon transformation. *Soil Biology and Biochemistry*
651 40, 425-433.
- 652 Kweon, O., Kim, S.-J., Holland, R.D., Chen, H., Kim, D.-W., Gao, Y., Yu, L.-R., Baek, S.,
653 Baek, D.-H., Ahn, H., 2011. Polycyclic aromatic hydrocarbon metabolic network in
654 *Mycobacterium vanbaalenii* PYR-1. *Journal of Bacteriology* 193, 4326-4337.

- 655 Lee, K., Boufadel, M., Chen, B., Foght, J., Hodson, P., Swanson, S., Venosa, A., 2015. Expert
656 Panel Report on the Behaviour and Environmental Impacts of Crude Oil Released into Aqueous
657 Environments. Royal Society of Canada, Ottawa, ON, Canada, ISBN: 978-1-928140-02-3.
- 658 Lewis, J., Martel, R., Trépanier, L., Ampleman, G., Thiboutot, S., 2009. Quantifying the
659 transport of energetic materials in unsaturated sediments from cracked unexploded ordnance.
660 *Journal of Environmental Quality* 38, 2229-2236.
- 661 Li, X., Fan, F., Zhang, B., Zhang, K., Chen, B., 2018. Biosurfactant enhanced soil
662 bioremediation of petroleum hydrocarbons: design of experiments (DOE) based system
663 optimization and phospholipid fatty acid (PLFA) based microbial community analysis.
664 *International Biodeterioration & Biodegradation* 132, 216-225.
- 665 Liao, J., Wang, J., Huang, Y., 2015. Bacterial community features are shaped by geographic
666 location, physicochemical properties, and oil contamination of soil in main oil fields of China.
667 *Microbial Ecology* 70, 380-389.
- 668 Liu, Q., Tang, J., Gao, K., Gurav, R., Giesy, J.P., 2017. Aerobic degradation of crude oil by
669 microorganisms in soils from four geographic regions of China. *Scientific Reports* 7, 1-12.
- 670 Mahmoudi, N., Beaupré, S.R., Steen, A.D., Pearson, A., 2017. Sequential bioavailability of
671 sedimentary organic matter to heterotrophic bacteria. *Environmental Microbiology* 19, 2629-
672 2644.
- 673 Mahmoudi, N., Fulthorpe, R.R., Burns, L., Mancini, S., Slater, G.F., 2013a. Assessing microbial
674 carbon sources and potential PAH degradation using natural abundance ¹⁴C analysis.
675 *Environmental Pollution* 175, 125-130.
- 676 Mahmoudi, N., Porter, T.M., Zimmerman, A.R., Fulthorpe, R.R., Kasozi, G.N., Silliman, B.R.,
677 Slater, G.F., 2013b. Rapid degradation of deepwater horizon spilled oil by indigenous microbial
678 communities in louisiana saltmarsh sediments. *Environmental Science and Technology* 47,
679 13303-13312.
- 680 Margesin, R., Hammerle, M., Tschërko, D., 2007. Microbial activity and community
681 composition during bioremediation of diesel-oil-contaminated soil: Effects of hydrocarbon
682 concentration, fertilizers, and incubation time. *Microbial Ecology* 53, 259-269.
- 683 McGuire, J.T., Cozzarelli, I.M., Bekins, B.A., Link, H., Martinović-Weigelt, D., 2018. Toxicity
684 assessment of groundwater contaminated by petroleum hydrocarbons at a well-characterized,
685 aged, crude oil release site. *Environmental Science & Technology* 52, 12172-12178.
- 686 McMurdie, P.J., Holmes, S., 2013. phyloseq: an R package for reproducible interactive analysis
687 and graphics of microbiome census data. *PLoS ONE* 8, e61217.
- 688 NRCan, 2020. Natural Resources Canada. Crude oil facts. <https://www.nrcan.gc.ca/our-natural-resources/energy-sources-distribution/fossil-fuels/crude-oil/what-are-oil-sands/18089>.
689
- 690 O'Leary, W., Wilkinson, S., Ratledge, C., 1988. Microbial lipids.

- 691 Oksanen, J., Blanchet, F.G., Kindt, R., Legendre, P., Minchin, P.R., O'hara, R., Simpson, G.L.,
692 Solymos, P., Stevens, M.H.H., Wagner, H., 2013. Package 'vegan'. Community ecology
693 package, version 2, 1-295.
- 694 Owens, E., Taylor, E., Marty, R., Little, D., 1993. An inland oil spill response manual to
695 minimize adverse environmental impacts, International Oil Spill Conference. American
696 Petroleum Institute, pp. 105-109.
- 697 Pérez-Pantoja, D., Donoso, R., Agulló, L., Córdova, M., Seeger, M., Pieper, D.H., González, B.,
698 2012. Genomic analysis of the potential for aromatic compounds biodegradation in
699 Burkholderiales. *Environmental Microbiology* 14, 1091-1117.
- 700 Pernar, N., Baksic, D., Antonic, O., Grubescic, M., Tikvic, I., Trupcevic, M., 2006. Oil residuals
701 in lowland forest soil after pollution with crude oil. *Water, Air, and Soil Pollution* 177, 267-284.
- 702 Podgorski, D.C., Zito, P., Kellerman, A.M., Bekins, B.A., Cozzarelli, I.M., Smith, D.F., Cao, X.,
703 Schmidt-Rohr, K., Wagner, S., Stubbins, A., 2021. Hydrocarbons to carboxyl-rich alicyclic
704 molecules: A continuum model to describe biodegradation of petroleum-derived dissolved
705 organic matter in contaminated groundwater plumes. *Journal of Hazardous Materials* 402,
706 123998.
- 707 Radović, J.R., Oldenburg, T.B., Larter, S.R., 2018. Environmental Assessment of Spills Related
708 to Oil Exploitation in Canada's Oil Sands Region, Oil Spill Environmental Forensics Case
709 Studies. Elsevier, pp. 401-417.
- 710 Rodgers-Vieira, E.A., Zhang, Z., Adrion, A.C., Gold, A., Aitken, M.D., 2015. Identification of
711 anthraquinone-degrading bacteria in soil contaminated with polycyclic aromatic hydrocarbons.
712 *Applied and Environmental Microbiology* 81, 3775-3781.
- 713 Schreiber, L., Fortin, N., Tremblay, J., Wasserscheid, J., Elias, M., Mason, J., Sanschagrín, S.,
714 Cobanlı, S., King, T., Lee, K., 2019. Potential for microbially mediated natural attenuation of
715 diluted bitumen on the coast of British Columbia (Canada). *Applied and Environmental*
716 *Microbiology* 85, e00086-00019.
- 717 Schreiber, L., Fortin, N., Tremblay, J., Wasserscheid, J., Sanschagrín, S., Mason, J., Wright,
718 C.A., Spear, D., Johannessen, S.C., Robinson, B., 2021. In situ microcosms deployed at the coast
719 of British Columbia (Canada) to study dilbit weathering and associated microbial communities
720 under marine conditions. *FEMS Microbiology Ecology* 97, fiab082.
- 721 Sizova, M., Panikov, N., 2007. *Polaromonas hydrogenivorans* sp. nov., a psychrotolerant
722 hydrogen-oxidizing bacterium from Alaskan soil. *International journal of systematic and*
723 *evolutionary microbiology* 57, 616-619.
- 724 Slater, G.F., White, H.K., Eglinton, T.I., Reddy, C.M., 2005. Determination of microbial carbon
725 sources in petroleum contaminated sediments using molecular ¹⁴C analysis. *Environmental*
726 *Science & Technology* 39, 2552-2558.

- 727 Spalding, R.F., Hirsh, A.J., 2012. Risk-Managed Approach for Routing Petroleum Pipelines:
728 Keystone XL Pipeline, Nebraska. *Environmental Science & Technology* 46, 12754-12758.
- 729 Stoyanovich, S.S., Yang, Z., Hanson, M., Hollebone, B.P., Orihel, D.M., Palace, V., Rodriguez-
730 Gil, J.L., Faragher, R., Mirnaghi, F.S., Shah, K., 2019. Simulating a spill of diluted bitumen:
731 environmental weathering and submergence in a model freshwater system. *Environmental*
732 *Toxicology and Chemistry* 38, 2621-2628.
- 733 Stuiver, M., Polach, H.A., 1977. Discussion: Reporting of ^{14}C data. *Radiocarbon* 19, 355-363.
- 734 Utting, N., Namsechi, B., McMullen, C., Brydie, J., Ahad, J.M.E., 2022. Comparing simulated
735 shallow subsurface spills of diluted bitumen and conventional crude oil. *Journal of Contaminant*
736 *Hydrology* 251, 104099.
- 737 Vestal, J.R., White, D.C., 1989. Lipid analysis in microbial ecology. *BioScience* 39, 535-541.
- 738 Vet, R., Artz, R.S., Carou, S., Shaw, M., Ro, C.-U., Aas, W., Baker, A., Bowersox, V.C.,
739 Dentener, F., Galy-Lacaux, C., 2014. A global assessment of precipitation chemistry and
740 deposition of sulfur, nitrogen, sea salt, base cations, organic acids, acidity and pH, and
741 phosphorus. *Atmospheric Environment* 93, 3-100.
- 742 White, D.C., Davis, W.M., Nickels, J.S., King, J.D., Bobbie, R.J., 1979. Determination of the
743 sedimentary microbial biomass by extractable lipid phosphate. *Oecologia* 40, 51-62.
- 744 Wickham, H., 2011. ggplot2. *WIREs Computational Statistics*, 3 (2), 180–185.
- 745 Widdel, F., Knittel, K., Galushko, A., 2010. Anaerobic hydrocarbon-degrading microorganisms:
746 an overview. *Handbook of hydrocarbon and lipid microbiology*, 1998-2022.
- 747 Wilkinson, S., Ratledge, C., 1988. *Microbial lipids*. Academic Press.
- 748 Yang, S., Wen, X., Shi, Y., Liebner, S., Jin, H., Perfumo, A., 2016. Hydrocarbon degraders
749 establish at the costs of microbial richness, abundance and keystone taxa after crude oil
750 contamination in permafrost environments. *Scientific Reports* 6, 1-13.
- 751 Zemo, D.A., Patterson, T.J., Kristofco, L., Mohler, R.E., O'Reilly, K.T., Ahn, S., Devine, C.E.,
752 Magaw, R.I., Sihota, N., 2022. Complex mixture toxicology: Evaluation of toxicity to freshwater
753 aquatic receptors from biodegradation metabolites in groundwater at a crude oil release site,
754 recent analogous results from other authors, and implications for risk management. *Aquatic*
755 *Toxicology* 250, 106247.
- 756 Zhao, J., Verma, M., Verter, V., 2020. Pipeline transportation of crude oil in Canada:
757 Environmental risk assessment using modified diffusion models. *Human and Ecological Risk*
758 *Assessment: An International Journal* 27, 1206-1226.
- 759
760
761
762

763 **Figure Headings**

764

765 **Figure 1.** Relative abundance distributions (mole percentage) of 12 of the most abundant PLFAs
766 in samples collected from the top, middle and bottom sampling depths during the 104-day exposure
767 period to dilbit and conventional crude.

768

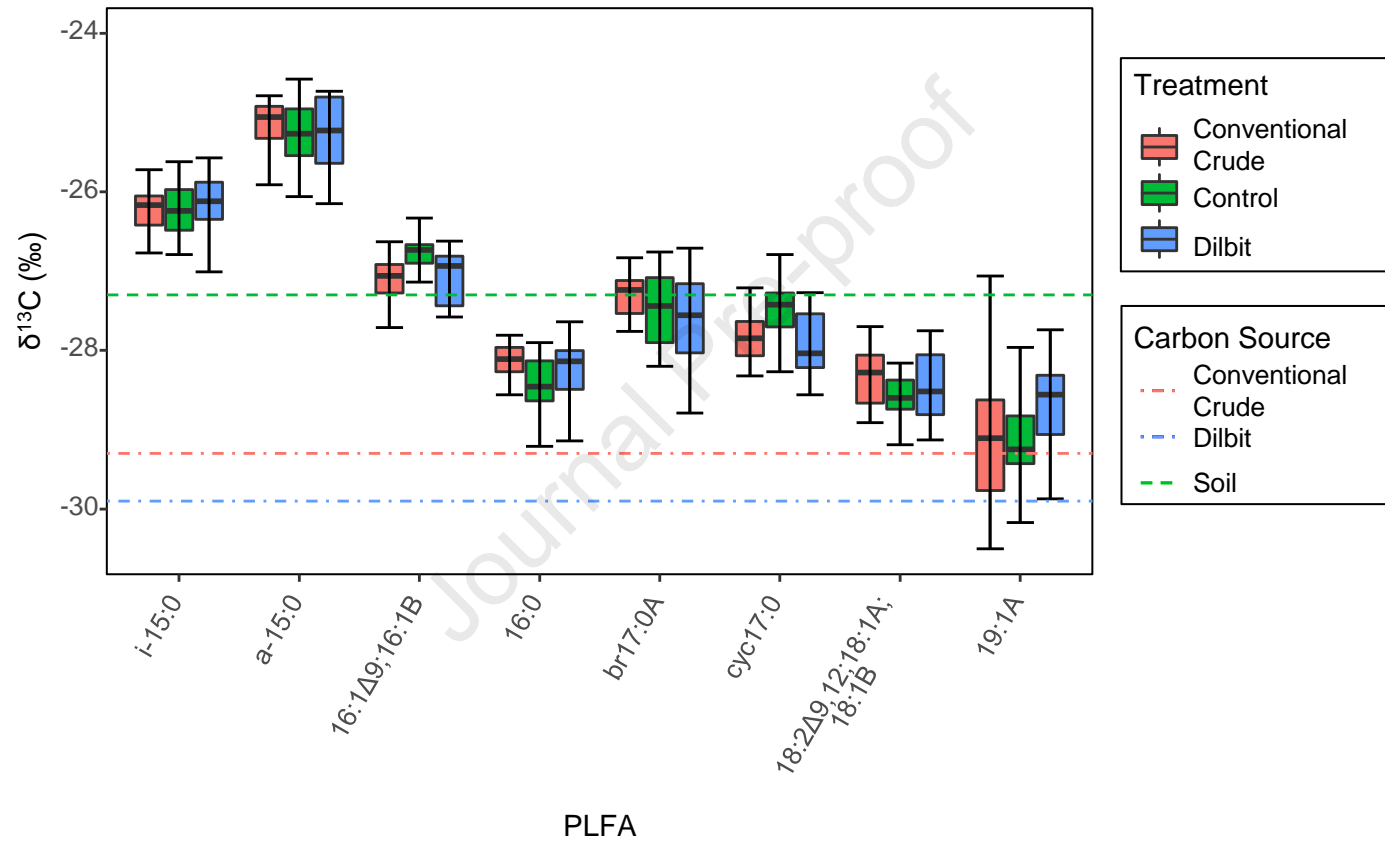
769 **Figure 2.** The average stable carbon isotope ($\delta^{13}\text{C}$) values for the most abundant PLFAs over the
770 course of the entire 104-day experiment. Error bars represent standard deviations between samples.
771 Outlier points are not shown but were included in calculations. The horizontal lines denote the
772 $\delta^{13}\text{C}$ values of the potential carbon sources: conventional crude (red; -29.3‰), dilbit (blue; -
773 29.9‰) and soil TOC (green; -27.3‰).

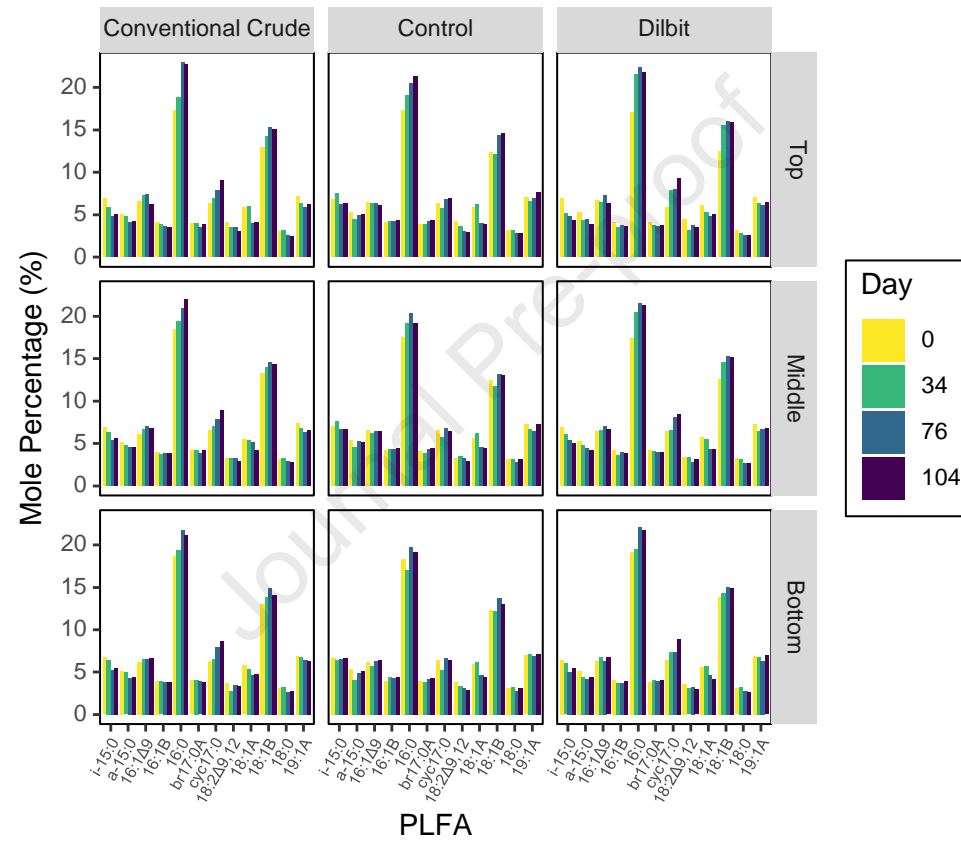
774

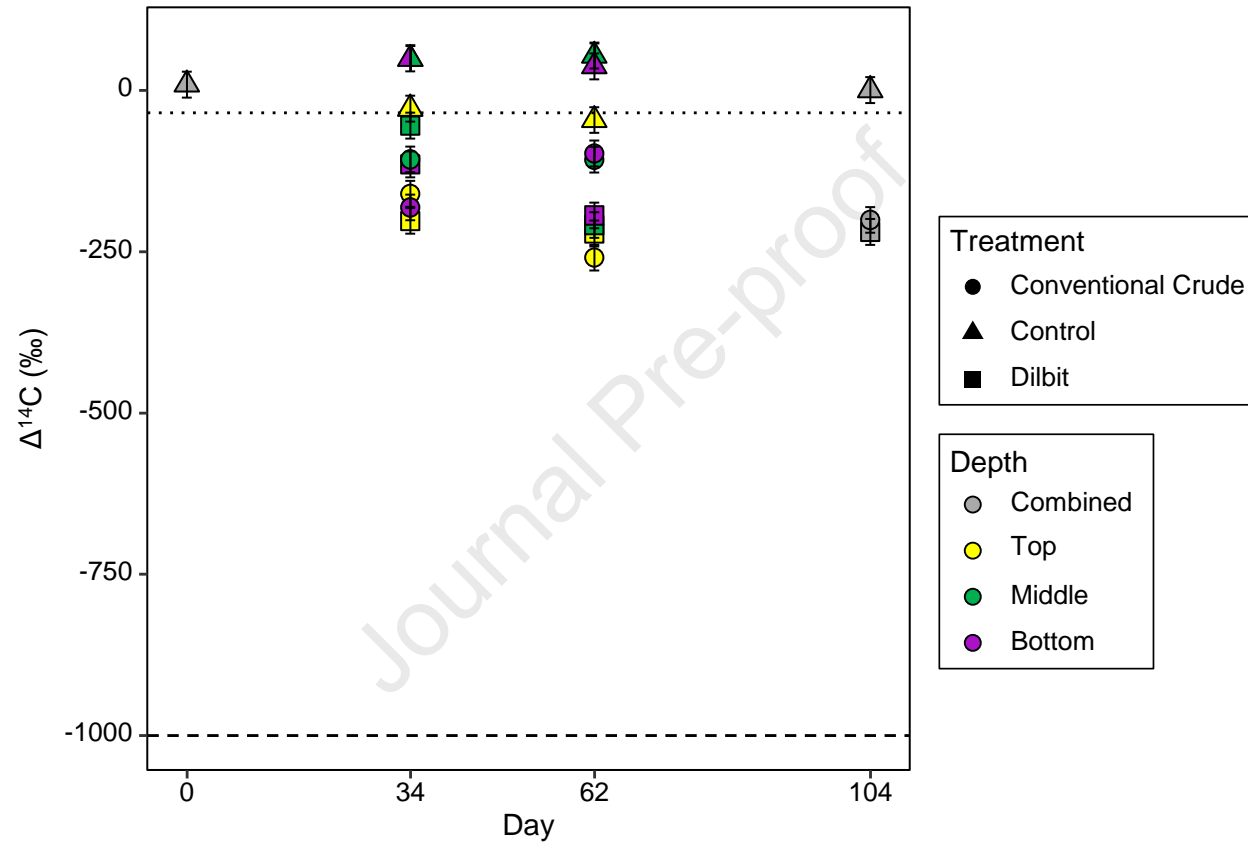
775 **Figure 3.** Radiocarbon ($\Delta^{14}\text{C}$) values for PLFAs at days 0, 34, 62, and 104. Top, middle, and
776 bottom sampling depths were combined for Days 0 (control) and 104 (control, dilbit and
777 conventional heavy crude). Top, middle, and bottom sampling depths were analysed individually
778 for Days 34 and 64 samples. The dotted line represents the $\Delta^{14}\text{C}$ value of the soil TOC (-35‰)
779 while the dashed line represents the $\Delta^{14}\text{C}$ value of dilbit and conventional heavy crude (-1000‰).
780 Error bars represent $\pm 20\%$ accuracy and precision of $\Delta^{14}\text{C}$ measurements.

781

782 **Figure 4.** Microbial community composition at the genus level. Relative abundances are expressed
783 as a percent (%). Facets group column treatments (top x-axis), and depths (y-axis). Genera with
784 an average relative abundance less than 1.5% are collectively labelled as 'Other'. Significant
785 increases in the abundance of *Polaromonas* were observed over time for both the dilbit and
786 conventional crude columns.







Highlights

- Controlled vadose zone spill experiments carried out using large soil-filled columns.
- Dilbit (DB) & conventional heavy crude (CC) showed similar biodegradation over 104 d.
- Up to ~ 20% of carbon in microbial phospholipid fatty acids derived from CC or DB.
- Abundances of *Polaromonas*, a known hydrocarbon-degrader, increased over time.
- Natural attenuation potential for DB similar to CC following a vadose zone spill.

Author statement

Leah M. Mindorff: Writing – original draft, Formal analysis, Investigation, Methodology;
Nagissa Mahmoudi: Conceptualization, Funding acquisition, Supervision, Writing – review & editing, Resources; **Scott L. J. Hepditch:** Formal analysis, Investigation, Methodology, Writing – review & editing; **Valerie S. Langlois:** Conceptualization, Writing – review & editing; **Samrat Alam:** Formal analysis, Writing – review & editing; **Richard Martel:** Conceptualization, Resources, Writing – review & editing; **Jason M. E. Ahad:** Conceptualization, Funding acquisition, Supervision, Writing – review & editing, Project administration, Resources.

Declaration of interests

The authors declare that they have no known competing financial interests or personal relationships that could have appeared to influence the work reported in this paper.

The authors declare the following financial interests/personal relationships which may be considered as potential competing interests:

Journal Pre-proof